Crystal clear insights into how the dynein motor moves

Andrew P. Carter
Medical Research Council Laboratory of Molecular Biology, Francis Crick Avenue, Cambridge CB2 0QH, UK
cartera@mrc-lmb.cam.ac.uk

Journal of Cell Science 126, 705–713

doi: 10.1242/jcs.120725

Summary

Dyneins are motor proteins that move along microtubules. They have many roles in the cell. They drive the beating of cilia and flagella, move cargos in the cytoplasm and function in the mitotic spindle. Dyneins are large and complex protein machines. Until recently, the way they move was poorly understood. In 2012, two high-resolution crystal structures of the >2500-amino-acid dynein motor domain were published. This Commentary will compare these structures and integrate the findings with other recent studies in order to suggest how dynein works. The dynein motor produces movement in a manner that is distinct from myosin and kinesin, the other cytoskeletal motors. Its powerstroke is produced by ATP-induced remodelling of a protein domain known as the linker. It binds to microtubules through a small domain at the tip of a long stalk. Dynein communicates with the microtubule-binding domain by an unconventional sliding movement of the helices in the stalk coiled-coil. Even the way the two motor domains in a dynein dimer walk processively along the microtubule is unusual.

Key words: Microtubule, Cytoskeleton, Motor protein, Dynein, Transport, ATPases associated with various activities (AAA+)

Introduction

The size of eukaryotic cells and the crowded nature of their cytoplasm mean that they rely on motor proteins to move components around. There are three families of cytoskeletal motor proteins, each defined by a conserved motor domain that hydrolyses ATP and generates movement. Myosins (Odronitz and Kollmar, 2007) move on actin filaments, whereas kinesins (Miki et al., 2005) and dyneins (Wickstead and Gull, 2007) move along microtubules. The three families have many members with different functions. Their representative structures are shown in Fig. 1. There are nine dynein subfamilies (Wickstead and Gull, 2007), all of which move towards the minus end of microtubules. Seven subfamilies are axonemal dyneins, which slide microtubules past each other to generate the beating motion of cilia and flagella. The other two dynein subfamilies transport cargos. Intraflagella transport (IFT) dynein (also known as dynein 1B and cytoplasmic dynein 2) moves components in the axoneme (Cole, 2003). Cytoplasmic dynein 1 (referred to here as cytoplasmic dynein) performs the majority of the minus-end-directed transport in the rest of the cell in most eukaryotes (Vale, 2003). It carries many different cargos, including mRNAs, membrane vesicles, aggregated proteins and whole nuclei (Allan, 2011). It also has many roles in mitosis (Vaughan, 2012). How cytoplasmic dynein carries out so many functions is only partially understood (Allan, 2011) but might be related to its complexity. Like all dyneins, cytoplasmic dynein is a multiprotein complex consisting of the motor-containing heavy chain and multiple accessory chains (see Fig. 1C). In addition, cytoplasmic dynein transport requires many other components, including the cofactor dynactin, regulators such as Lissencephaly-1 (Lis1, also known as PAFAH1B1) and multiple adaptors (Kardon and Vale, 2009).

The common feature of all dyneins is a heavy chain with a conserved, ~3000-amino-acid long, motor domain at its C-terminus (Fig. 2A,B). Although kinesin and myosin belong to the G-protein superfamily (Kull et al., 1998), the dynein motor domain is part of the AAA+ superfamily (ATPases associated with various activities). AAA+ proteins are typically hexameric rings that remodel protein substrates, break up filaments and unwind proteins or nucleic acids (Neuwald et al., 1999). Dynein is one of only two proteins, in which six AAA+ domains are linked together in a single protein [the other is the ribosome biogenesis factor Rea1, also called midasin (Bassler et al., 2010)]. In dynein, four of the AAA+ domains bind nucleotides. The size of the dynein motor domain, the presence of multiple nucleotide-binding sites and the fact that dynein only has a distant relationship to kinesin and myosin suggest that dynein uses a number of unique mechanisms to generate movement. In this Commentary, I will discuss how the first high-resolution crystal structures of the dynein motor domain (Kon et al., 2012; Schmidt et al., 2012), together with other studies, have begun to shed light on the way dynein uses its AAA+ domains to move along microtubules. Understanding how the motor works will aid future cell biology studies of dynein, especially those that address the regulation of transport.

Structural features of dynein

The gross features of dynein were identified by sequence analysis and electron microscopy (Gee et al., 1997; Samsó et al., 1998; Neuwald et al., 1999; Burgess et al., 2003; Roberts et al., 2009) (Fig. 2). At the N-terminus of the dynein heavy chain is the tail, which is the site of multimerisation and cargo interaction (Fig. 1). It is followed by the linker domain, which spans a ring of AAA+ domains (Burgess et al., 2003; Roberts et al., 2009) (Fig. 2). The linker is the force-producing motile element that changes position in response to nucleotide (Burgess et al., 2003; Kon et al., 2005; Shima et al., 2006b). The motor binds microtubules through a small microtubule-binding domain (MTBD) that is located at the tip of a 15-nm-long antiparallel coiled-coil stalk (Gee et al., 1997; Koonce, 1997).

Journal of Cell Science

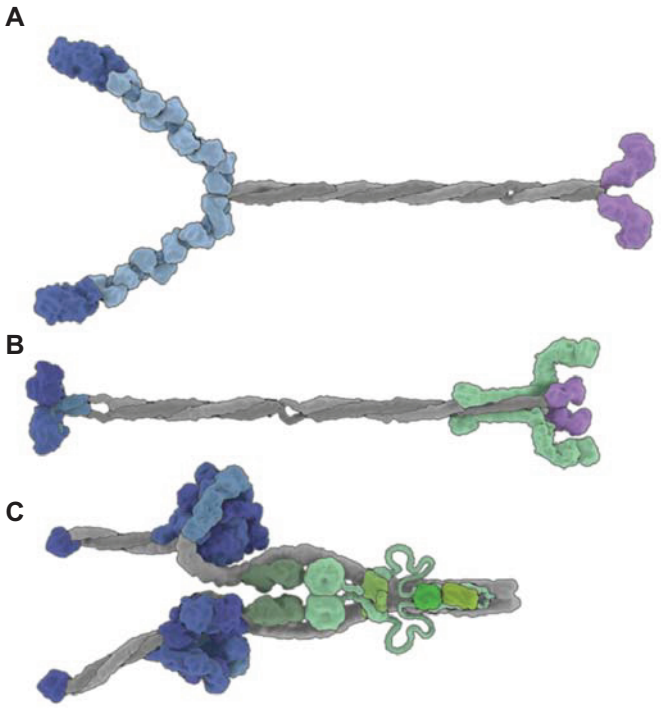

Fig. 1. Representative structures of the three families of cytoskeletal motor proteins. The structures are shown to scale. (**A**) Myosin V. Myosins are actin motors. Myosin V is a dimeric protein that can walk for multiple steps along an actin filament (processive motion) and is involved in vesicle transport (Vale, 2003). The motor domain (dark blue) of myosins belong to the G-protein superfamily. It couples hydrolysis of ATP to alternating cycles of actin binding and conformational changes in the motile element called the lever arm. The lever arm consists of a helix wrapped with calmodulin light chains (light blue). The motor domains are dimerised through a coiled-coil (grey) domain, and the cargo-binding tail (purple) is at the C-terminal end of the motor. Image generated from the Protein Data Bank (PDB) IDs 2DFS (myosin motor domain), 3MMI (tail) and 1GK4 (coiled-coil). (**B**) Kinesin-1 (KIF5). Kinesins are microtubule motors. Most family members, including kinesin-1, move towards the plus end of microtubules, although the kinesin-14 family motors move in the other direction, towards the minus end. Kinesin-1 is a processive motor involved in vesicle and mRNA transport (Vale, 2003). The motor domain (dark blue) is structurally related to the myosin motor domain and the motile element is a short peptide called the neck linker (light blue). The motor domains are dimerised through a coiled-coil (grey). Cargo binding is mediated by the kinesin tail (purple) and kinesin light chains (green). Image generated using PDB IDs 3KIN (motor domain), 3NF1 (globular part of light chain) and 1GK4 (coiled-coil). (**C**) Cytoplasmic dynein. Motors of the dynein family all move towards the minus end of microtubules. Cytoplasmic dynein is a processive dimeric motor responsible for almost all the minus-end-directed microtubule movement in a cell. The dynein motor binds microtubules through a microtubule-binding domain (MTBD) at the end of a coiled-coil stalk (grey). The motor domain consists of a ring of AAA+ domains (dark blue) with between one and three active sites of ATP hydrolysis. The motile element is the linker (light blue), which reaches across the face of the AAA+ ring. The N-terminal tail of dynein (grey) is involved in dimerisation and binding to dimers of intermediate chains, light intermediate chains and three light chains (different shades of green). Cargo binding is mediated by these accessory chains. The structure elements were generated using PDB IDs 4AKG (motor domain), 3ERR (MTBD), 1GK4 (stalk coiled-coil), and 3L9K, 3FM7 and 3KCI (light chains). The rest of the model, including the heavy chain tail (grey), intermediate chain and light intermediate chain (green), is an artist's impression. Figure prepared by Janet Iwasa (Department of Biochemistry, University of Utah, UT).

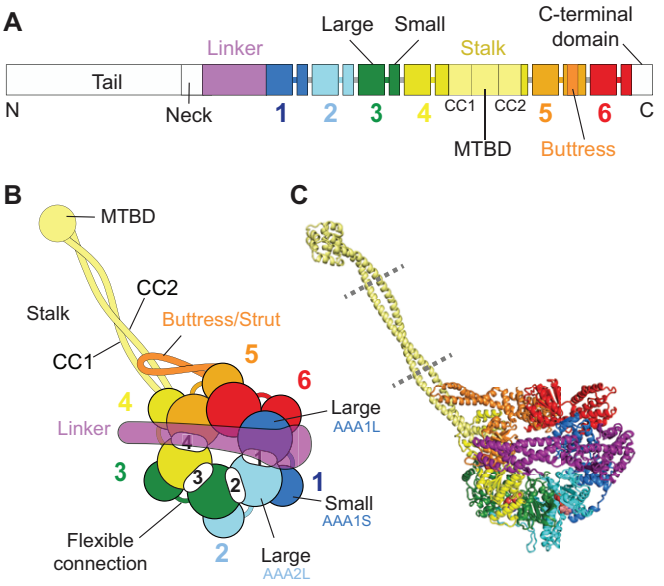

Fig. 2. Architecture of the dynein motor. (**A**) Schematic illustration of a dynein heavy chain domain structure, including the N-terminal tail (see Fig. 1), the linker and the six AAA+ domains (labelled 1–6). Each AAA+ domain is split into a large (L) and small (S) subdomain. The position of the stalk, microtubule-binding domain (MTBD) and buttress are indicated. The C-terminal domain is not present in yeast dynein. (**B**) Cartoon of the dynein motor domain showing the linker domain that stretches across a ring of six AAA+ domains. The four nucleotide-binding sites (shown as white ovals and numbered in black: AAA1 site as 1, etc.) are located between the AAA+ domains. The large and small submodules of each AAA+ domain are linked by a flexible connection. The small domain packs against the large domain of the neighbouring AAA+. The stalk, with the MTBD at its end, emerges from the small domain of AAA4. It is supported by a coiled-coil from the small domain of AAA5, called the buttress. (**C**) Model of the dynein motor domain that has been constructed using the yeast motor domain (PDB ID 4AKG), an artificial length of coiled-coil (between the dotted lines), and the MTBD of mouse cytoplasmic dynein (PDB ID 3ERR).

The first three-dimensional view of the motor domain structure was provided by two low-resolution X-ray crystal structures (Carter et al., 2011; Kon et al., 2011). These were shortly followed by high-resolution structures. In my laboratory, the structure of the yeast cytoplasmic motor domain, with a truncated stalk, has been solved to 3.3 Å in the absence of nucleotides (Schmidt et al., 2012). The structure of the *Dictyostelium discoideum* cytoplasmic dynein, with a truncated microtubule-binding domain, has also been solved to 2.8 Å in the presence of ADP, and that with a full-length stalk to 3.8 Å (Kon et al., 2012). The connection between the stalk and the MTBD is partially disordered in the 3.8 Å structure. Therefore, a model of the whole dynein motor domain in Fig. 2C was constructed using the separately solved motor and MTBD domains. These crystal structures provide new insights into how the motor converts ATP hydrolysis into movement. The sections below will describe the motor domain structure and the following sections will discuss its function.

The linker

The dynein linker is functionally equivalent to the lever arm in myosin and the neck linker in kinesin (Vale and Milligan, 2000). It is made up of a series of subdomains, consisting mainly of

bundles of α-helices (Fig. 3A). Some subdomains (e.g. 1 and 3) also contain β-sheet components. Long α-helices run between the subdomains in an arrangement similar to that found in the cytoskeletal protein spectrin (Grum et al., 1999). Subdomains 1 and 2 span across the top face of the AAA+ ring. Subdomains 3 and 4 run down the side of the ring next to the first AAA+ domain (AAA1). The contacts between subdomains 2 and 3 are less extensive than those between other subdomains. This interface between subdomains 2 and 3 is called the cleft (Kon et al., 2012; Schmidt et al., 2012) and might be the hinge that allows the linker to move (Fig. 3A).

The AAA+ ring

The dynein linker is followed in the protein sequence by six AAA+ domains (AAA1–AAA6) that form a clockwise ring (as viewed in Fig. 2B). Each AAA+ domain is divided into a 'large' (or 'α/β') and a 'small' (or 'α') subdomain, joined by a flexible connection (Fig. 2A,B; Fig. 3B). The large subdomains (e.g. AAA1L–AAA6L) form the top surface of the AAA+ ring, closest to the linker (Fig. 2B). In common with other AAA+ proteins, most of the large domains of dynein contain peptide 'inserts' in their conserved core (Fig. 3B). These inserts line the top surface of the AAA+ ring. The interaction of the inserts in AAA2 with the linker play a key role in dynein motility as discussed below. The role of the inserts in the other AAA+ domains is unclear.

The small subdomains in dynein (AAA1S–AAA6S) lie on the bottom face of the ring (Fig. 2B). Small domains of AAA+ proteins are variable in structure, although they often contain a bundle of α-helices (Erzberger and Berger, 2006). In dynein, all the small domains contain a structurally similar bundle of five α-helices (Fig. 3B). This similarity implies that the AAA+ domains in dynein are more closely related to each other than to any other AAA+ protein. This suggests they evolved by duplication of an ancestral AAA+ domain. The small submodule of one domain (e.g. AAA1S) packs in against the large submodule of the neighbouring domain (e.g. AAA2L) (Fig. 3B) and this packing interaction is similar to that observed in other AAA+ proteins (Bochtler et al., 2000; Glynn et al., 2009; Carter et al., 2011).

The nucleotide-binding sites are found between adjacent AAA+ domains (Fig. 2B; Fig. 3C). In dynein, the binding sites are named after the AAA+ domain that contributes the conserved Walker A and B motifs. Therefore the 'AAA1 site' (also referred to as 'P1' in the literature) is found between AAA1 and AAA2. Nucleotides bind to dynein at four sites (AAA1, AAA2, AAA3 and AAA4), which are discussed below.

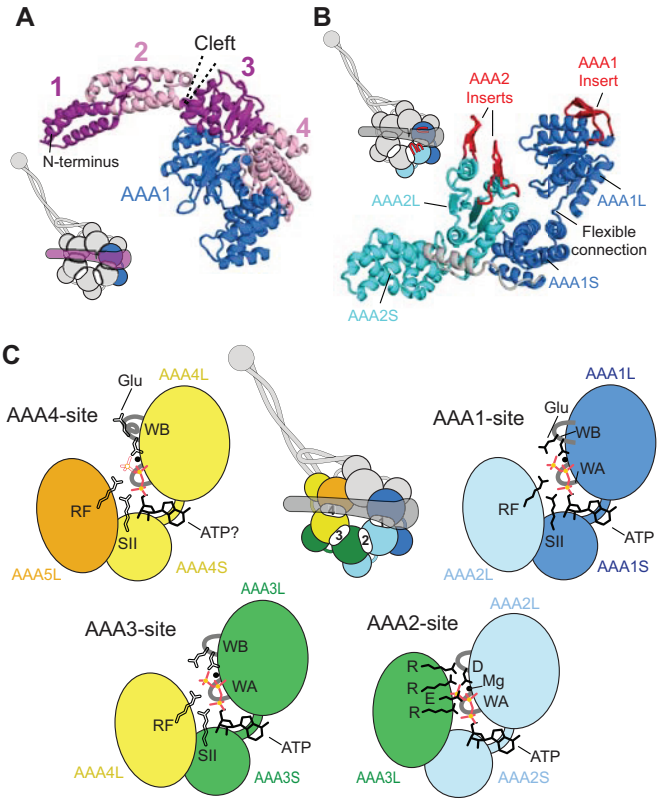

Fig. 3. Components of the motor domain. (**A**) The dynein linker is made up of four subdomains (1–4) coloured alternately in dark and light purple. Subdomains 3 and 4 interact with AAA1. The interface between subdomains 2 and 3 is a cleft that might act as a hinge. (**B**) AAA+ domains are made up of a large (L) and small (S) subdomain, linked by a flexible connection. The small subdomain (AAA1S) packs against the neighbouring large subdomain (AAA2L). The AAA+ domains contain different inserts (red) in their conserved large subdomains. (**C**) Schematic illustration of the four nucleotide-binding sites in dynein. Residues that are important for nucleotide binding are shown in black (solid black, conserved among all dyneins; black outline, conserved in only a subset of dyneins). Details are described in the text. WA, Walker A motif; WB, Walker B motif; Glu, catalytic glutamate; SII, sensor II arginine; RF, arginine finger; Mg, magnesium ion coordinated with ATP and ADP. In AAA2, the residues involved in electrostatic interactions are labelled. R, arginine; E, glutamate; D, aspartate. In AAA4, a turn of α-helix after the WB angles the catalytic glutamate away from the nucleotide.

The stalk

The dynein stalk consists of a pair of helices (CC1 and CC2) that emerge from AAA4S and wrap around each other to form an antiparallel coiled-coil (Fig. 2B,C). At the tip of the stalk is the MTBD that consists of a small bundle of helices (Carter et al., 2008). At its base, the stalk is contacted by an antiparallel pair of helices, called the buttress (Carter et al., 2011) or strut (Kon et al., 2011), that emerge from AAA5S. The buttress is likely to provide support to the base of the stalk and may also play a role in the communication of the ATP state of the AAA+ ring to the MTBD.

Roles of the nucleotide-binding sites

AAA1 site

AAA1 is the 'main' site for ATP hydrolysis. It contains all the residues AAA+ proteins use to bind and hydrolyse ATP (Wendler et al., 2012) (Fig. 3C), and is the only site where residues are conserved among all dyneins. It is also the only site at which mutation of catalytic residues completely abolishes motility (Kon et al., 2004; Kon et al., 2005). The adenine base is deeply buried in a pocket between AAA1L and AAA1S. The ATP phosphates are contacted by the Walker A (or P-loop) motif on AAA1L and the sensor-II (SII) arginine from AAA1S. Residues that are involved in catalysis include a catalytic glutamate in the Walker B (WB) motif and an arginine finger (RF) from AAA2L. The active site residues progressively close in around ATP as it first binds and is then hydrolysed. This in turn closes the gap between AAA1L and AAA2L. The ways in which this motion is coupled to the mechanochemistry of dynein, are discussed below.

AAA2 site

The crystal structure of yeast dynein, solved in the absence of added ATP or ADP, still contains nucleotide bound at AAA2. This nucleotide must have co-purified with the protein and hence is very tightly bound (Schmidt et al., 2012). The resolution of the yeast structure is not high enough to distinguish whether it is an ADP or ATP molecule. In the *Dictyostelium* structure, the nucleotide at AAA2 was originally modelled as ADP (Kon et al., 2012). When we re-refined the deposited data (H. Schmidt and A. P. C., unpublished), however, we found it is more likely that *Dictyostelium* dynein contains ATP at AAA2. The ATP and its magnesium ion form part of a network of electrostatic interactions (Fig. 3C) between charged residues (i.e. arginine, glutamate and aspartate residues) that keep the interface between AAA2L and AAA3L tightly closed. This means that when the AAA1 site closes around ATP, AAA2L and AAA3L move together as a rigid block.

AAA3 site

The AAA3 site contains all the residues that are required for ATP hydrolysis in cytoplasmic dyneins, but it is not conserved in axonemal or IFT dyneins (Fig. 3C). Mutations in this site that block ATP binding (Kon et al., 2004) or hydrolysis (Kon et al., 2005; Cho et al., 2008) lead to a 95% decrease in motility of cytoplasmic dyneins. How could ATP hydrolysis at AAA3 be required for motor function? One possibility is that there is a two-stroke cycle in cytoplasmic dynein, with both AAA3 and AAA1 opening and closing, and with each unit hydrolysing ATP alternately. This would suggest that at least two ATP molecules are hydrolysed per step for which there is evidence both for and against (Reck-Peterson et al., 2006; Ross et al., 2006).

Another possibility is that the ATP at AAA3 forms part of a switch that allows the nucleotide state of AAA3 to control the activity of the AAA1 site. A tantalising hint that this is the case comes from recent work on Lis1 (Huang et al., 2012), a regulator of dynein that is required for many of its functions, including initiation of transport (Egan et al., 2012) and production of high forces (McKenney et al., 2010). Lis1 acts as a clutch that uncouples ATP hydrolysis from movement along the microtubule. In the presence of Lis1, ATP hydrolysis rates are high, but dynein movement along the microtubule is slow and highly processive (Huang et al., 2012). Lis1 also binds right next to AAA3 and AAA4 (Huang et al., 2012), which suggests that it could uncouple any communication between AAA1 and the base of the stalk by influencing one or both of these sites.

AAA4 site

The role of ATP hydrolysis at the AAA4 site is even more mysterious than that at AAA3. The AAA+ catalytic residues are poorly conserved in axonemal, IFT and fungal cytoplasmic dyneins, suggesting hydrolysis is not required in these dyneins (Fig. 3C). In support of this idea, the yeast motor domain crystal is able to bind ADP but not the non-hydrolysable ATP analogue AMPPNP or ATP itself (Schmidt et al., 2012). In contrast, AAA4 in other cytoplasmic dyneins contains all the catalytic residues. Furthermore, AAA4 in dynein from *Dictyostelium* has ATPase activity when all the other ATPase sites are mutated (Kon et al., 2012). Confusingly, however, in AAA4 sites in both yeast and *Dictyostelium*, a helix directly after the Walker B motif angles the catalytic glutamate away from the nucleotide-binding pocket (Fig. 3C). This means an as yet unknown conformational change must occur for the *Dictyostelium* dynein AAA4 site to hydrolyse ATP.

Coupling ATP hydrolysis to dynein movement

At a basic level, the events that lead to dynein moving along the microtubule are well established (Kon et al., 2005) (Fig. 4A). First, dynein with ADP in AAA1 is bound to the microtubule with the linker in the post-powerstroke (unprimed) conformation, close to the base of the stalk. ADP is then released to leave a nucleotide-free motor. Second, ATP binds to the motor domain, which is followed by release of the MTBD from the microtubule and a movement of the linker to the pre-powerstroke (primed) position. Third, the motor diffuses to a new site on the microtubule. ATP is hydrolysed and a phosphate is released. Finally, rebinding to the microtubule is followed by the powerstroke, in which the linker returns to its position close to the stalk and the cycle can continue. The new X-ray crystal structures now allow us to understand how ATP drives these steps at a mechanistic level, as discussed in the following sections.

Changes between ADP-bound and nucleotide-free dynein

A comparison of the *Dictyostelium* (ADP-bound) (Kon et al., 2012) and yeast (nucleotide-free) (Schmidt et al., 2012) X-ray crystal structures raises the possibility that large conformational changes occur upon ADP release from dynein. Negative-stain electron microscopy previously showed that both ADP-bound and nucleotide-free dynein appear similar (Burgess et al., 2003; Roberts et al., 2009), and, indeed, the *Dictyostelium* and yeast crystal structures are superficially similar. In both structures, the linkers are in the post-powerstroke position close to the base of the stalk (Fig. 4B, insets). Viewed from the side, however, it is apparent that there are large movements in the AAA+ domains (Fig. 4B). These differences are most clearly seen in a movie (supplementary material Movie 1). In summary, during the transition from the *Dictyostelium* (ADP) to yeast (nucleotide-free) structure, the AAA1 site opens wide and allows the release of ADP (compare the middle and left panels of Fig. 4C). The block of AAA+ domains (AAA2L to AAA4L) move downwards (Fig. 4B; asterisks), before AAA5L swings over and closes the AAA4 site. This is accompanied by a large shift in the position of AAA6L (supplementary material Movie 1). The N-terminus of the linker docks onto a conserved site on AAA5L (Fig. 4B) and might help stabilise dynein in the nucleotide-free conformation.

Are the differences between the *Dictyostelium* and yeast crystal structures due purely to ADP release or to other differences between the motors? It will require crystal structures of the same dynein species in different nucleotide states to resolve this issue. Yeast dynein lacks a C-terminal domain found in *Dictyostelium* dynein (coloured grey in Fig. 4B) and this might contribute to the structural differences around AAA5 and AAA6. It appears likely, however, that the downwards movement of the block of AAA+ domains (AAA2L to AAA4L) is caused by ADP release. A recent cryo-EM structure of a nucleotide-free axonemal dynein (Roberts et al., 2012) shows a conformation that is similar to the yeast crystal structure (Schmidt et al., 2012). This demonstrates that the nucleotide-free conformation is neither induced by crystal packing nor is it a peculiarity of yeast dynein.

What role might large conformational changes on ADP release play in dynein? A clue comes from the observation that the

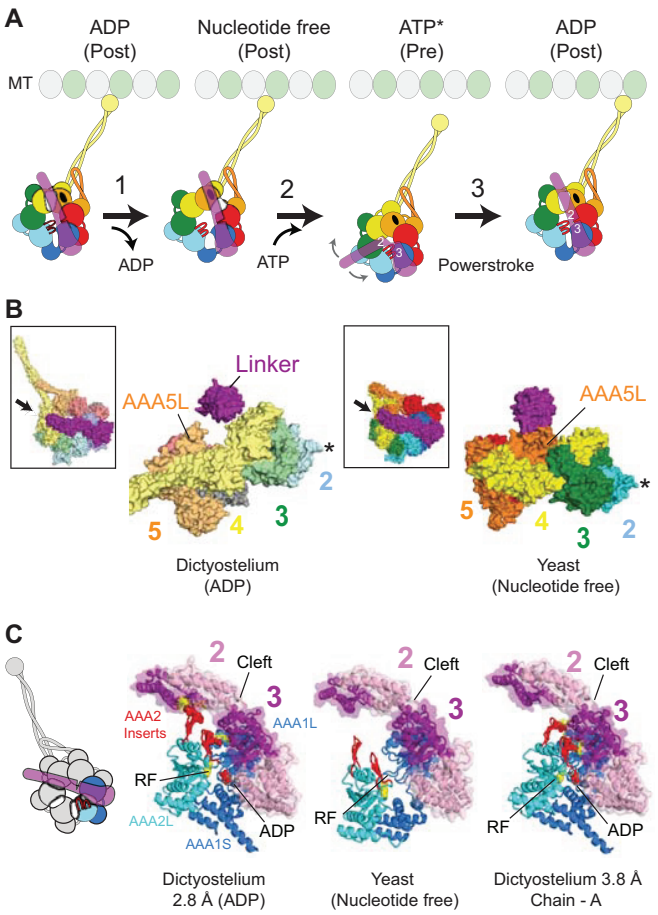

Fig. 4. Mechanical cycle of dynein. (**A**) Schematic illustration of the mechanical cycle of the dynein motor domain (see Fig. 1B for details of the motor domain). Step 1. ADP is released. The AAA+ ring undergoes conformational changes, but the motor remains bound to the microtubule (MT) with the linker in the post-powerstroke position. Step 2. ATP binding results in release from the microtubule, and the linker moves into a pre-powerstroke position. Step 3. The motor diffuses to a new position on the microtubule and rebinds. The linker undergoes a force-producing powerstroke to return to its original position. Further details are given in the text. (**B**) The ADP-bound *Dictyostelium* motor domain (PDB ID 3VKG) and the nucleotide-free yeast (*Saccharomyces cerevisiae*) motor domain (PDB ID 4AKG) both show their linkers in the post-powerstroke position, close to the base of the stalk (see insets; domains are coloured as in Fig. 2, with the yeast structure in bright colours and the *Dictyostelium* structure in paler colours). There are large conformational changes on ADP release, which are apparent when the structures are viewed from the side in the direction of the arrows shown in the insets. In the nucleotide-free structure, AAA5L moves over to contact the linker and a block of AAA+ domains (from AAA1S to AAA4L) move down (asterisks mark the movement of AAA2S with respect to AAA1L). Other changes can be observed in supplementary material Movie 1. (**C**) The AAA2 inserts change their interaction with the linker as the AAA1 site opens and closes. Left: in the 2.8 Å *Dictyostelium* ADP structure (PDB ID 3VKG), the AAA2 inserts make contact to multiple subdomains near the base of the cleft. Middle: in the nucleotide-free structure (PDB ID 4AKG), the inserts do not contact the linker. Right: in one of the copies (chain A) of the motor domain in the 3.8 Å ADP structure (PDB ID 3VKH), the AAA1 site has closed further and the inserts are both in contact with subdomain 3 of the linker (which remains in the post-powerstroke position). This conformation might occur between the post- and pre-powerstroke states of dynein (i.e. constitute a sub-step of step 2 shown in A). The arginine finger (RF) in the AAA1 site is too far from the ATP molecule to catalyse hydrolysis, suggesting AAA1 closes further. This closure might be responsible for driving the linker into the pre-powerstroke position.

nucleotide-free form of dynein in the crystal structure has a very low affinity for nucleotide at the AAA1 site (Schmidt et al., 2012). This suggests that this conformation might promote nucleotide exchange by ejecting the bound ADP. The nucleotide-free conformation can only exist transiently and must be in equilibrium with a conformation that has higher nucleotide affinity. As in the cell the concentration of ATP is higher than that of ADP, the net result of this equilibrium would be that ATP replaces ADP and the cycle of ATP hydrolysis continues.

This raises another question of why dynein needs an ADP ejection mechanism. The answer might lie in the fact that the adenine base in AAA+ proteins lies tightly buried in a pocket between the large and small domains. Release of ADP from AAA+ proteins might be too slow, unless a very low affinity conformation is part of the ATP hydrolysis cycle. Interestingly, the presence of very low affinity conformations has been observed in other AAA+ proteins. For example, structures of the unfoldase ClpX (Glynn et al., 2009) and biochemical studies on the PAN ATPase in the proteasome (Smith et al., 2011) show that nucleotides only bind to four of the six potential sites at a time, whereas the remaining two are held in a conformation where they cannot bind nucleotide.

Movement of the linker and the dynein powerstroke

The powerstroke of dynein involves movement of the linker (Burgess et al., 2003; Roberts et al., 2009). The two crystal structures (Kon et al., 2012; Schmidt et al., 2012) and a recent cryo-electron microscope study (Roberts et al., 2012) now suggest an explanation for how the linker moves. After ADP release, ATP binds to the motor domain causing the AAA1 site to close (see Step 2 in Fig. 4A). This brings the two β-hairpin 'inserts' in AAA2L into contact with the linker subdomain 3. The linker is 'remodelled', and the hinge-like cleft between linker subdomains 2 and 3 becomes flexible. The linker bends at the cleft to take up its pre-powerstroke. After ATP hydrolysis, the AAA1 site reopens (step 3 in Fig. 4A), the 'AAA2 inserts' are withdrawn and the linker snaps back to a straight conformation producing a powerstroke. In this post-powerstroke ADP-bound state, the AAA2 inserts contact the linker at a different site, straddling the base of the cleft (Kon et al., 2012).

The interface between subdomains 2 and 3 was identified as a probable hinge in the linker in both X-ray crystal structures (Kon et al., 2012; Schmidt et al., 2012). Unlike the other linker subdomain interfaces, it appears as a cleft with a single helix crossing at the base. Alignment of different motor domain structures on AAA1L (see supplementary material Movies 1, 2) provides evidence that the position at the N-terminal end of the linker (in subdomains 1 and 2) is variable and that the cleft at the subdomain 2 and 3 interface is the hinge about which they move. The AAA2 inserts and a patch of residues on the linker subdomain 3 are highly conserved, suggesting that they interact (Schmidt et al., 2012). Mutations in the AAA2 inserts prevent the movement of the linker to the pre-powerstroke position (Kon et al., 2012), suggesting they have a role in priming the linker for the powerstroke.

The dynein crystal structures all contain two independent copies of the motor domain. In the 2.8 Å crystals, the AAA2 inserts make the same contacts in both copies (Kon et al., 2012) (Fig. 4C, left panel). This interaction, which straddles the base of the cleft, might occur in the ADP-bound post-powerstroke state of dynein. In the 3.8 Å structure, one copy of the motor domain

shows a similar structure to those in the 2.8 Å structure (Kon et al., 2012). The other copy has been trapped with its AAA1 site more tightly closed and its AAA2 inserts contact subdomain 3 (Fig. 4C, right panel). This structure might correspond to the motor domain in an ATP-bound conformation just prior to the bending of the linker. In this conformation, the catalytic arginine finger (RF) in the AAA1 site is still not in the correct position for ATP hydrolysis to occur (Wendler et al., 2012). The movement of this arginine finger is presumably what causes the remodelling of the linker and allows it to move to its pre-powerstroke position.

Recent cryo-electron microscopy structures of dynein (Roberts et al., 2012) suggest that the interaction of the AAA2 inserts with the linker not only makes it bend but also results in it becoming flexible. The N-terminal end of the linker becomes disordered when the motor is trapped in the pre-powerstroke conformation. Despite the disorder, the linker has a preferred position, which the authors were able to identify by using a variance map. These maps show that the linker is bent at a position that corresponds to the cleft at the subdomain-2–subdomain-3 interface. These electron microscopy structures also indicate why the linker returns to the straight post-powerstroke position when the AAA1 site reopens (Roberts et al., 2012). When *Dictyostelium* dynein is truncated at its C-terminus, the linker frequently fully undocks from the AAA+ ring. The isolated linker is a defined and rigid structure, suggesting that it has to be actively remodelled to bend. Removal of the AAA2 inserts allows it to snap back into a straight conformation (Roberts et al., 2012).

In myosin and kinesin, small conformational changes in the ATP-binding pocket are amplified by a movement of the lever arm or the zipping down of the peptide neck-linker (Vale and Milligan, 2000). However, dynein uses a different mechanism. ATP binding causes a relatively large closure of the gap between AAA+ domains. This movement is amplified further by the active remodelling of a linker domain. Reopening of the gap between the AAA+ domains allows the linker to snap back into position. This mechanism might be similar to the way some other AAA+ proteins remodel their substrates. For example, parallels have been drawn with the protein PspF (Cho and Vale, 2012), which remodels the RNA-polymerase-binding σ factor (Rappas et al., 2005).

Release of dynein from microtubules upon ATP binding

ATP binding to AAA1 lowers the affinity of MTBD for microtubules, which allows dynein to detach and diffuse to its next binding site. Release occurs even in a monomeric dynein (Imamula et al., 2007), in which the AAA+ ring is only linked to the MTBD through the coiled-coil of α-helices in the stalk. How exactly this happens can be broken down into three parts, as discussed below.

Transmission of a signal along the coiled-coil stalk

Standard coiled-coils consist of two α-helices that wrap round each other. They are stabilised by a heptad repeat (abcdefg) in the protein sequence in which the first (a) and fourth (d) amino acids are predominantly hydrophobic. The ‘a’ and ‘d’ residues in one helix pack against those in the second helix to form the hydrophobic core of the coiled-coil. The current model for communication along the dynein stalk is that the first helix (CC1) slides by a half heptad with respect to the second helix (CC2) (Carter and Vale, 2010). This movement would change the packing in the core of the coiled-coil. Residues in the ‘d’ position in CC1 slide over to where the ‘a’ position residues were previously. The ‘a’ position residues move out of the core of the coiled-coil and become solvent exposed. A previously solvent-exposed residue moves into the core of the coiled-coil to occupy the space vacated by the ‘d’ position residue.

The ‘half heptad sliding’ model for dynein is supported by biochemical data (Gibbons et al., 2005; Carter et al., 2008; Kon et al., 2009). Half-heptad transitions have also been directly observed in other coiled-coils (Croasdale et al., 2011; Macheboeuf et al., 2011). Now, there is also structural evidence that they occur in dynein (Fig. 5A). A previous X-ray crystal structure of part of dynein’s stalk and its MTBD showed it trapped in a conformation with a low affinity for microtubules (Carter et al., 2008) (Fig. 5A, right panel). The 2.8 Å *Dictyostelium* structure (Kon et al., 2012) contains an overlapping region of the stalk (Fig. 5A, left panel). The stalk in *Dictyostelium* dynein is expected to be in a high-affinity conformation because the ADP-bound form of dynein binds tightly to microtubules. As predicted, the region of overlap between the two structures differs by a sliding of CC1 relative to CC2. The transition from the high-affinity (ADP) to the low-affinity (ATP) form of dynein involves a half-heptad movement of CC1 away from the AAA+ ring and towards the MTBD.

In a standard coiled-coil, a half-heptad shift would expose the hydrophobic ‘a’ position residues to solvent, which would be energetically very unfavourable. However, in the CC1 of dynein these ‘a’ positions are not hydrophobic, and only the ‘d’ positions are conserved as hydrophobic residues (Gibbons et al., 2005). This pattern of conservation is apparent in the stalk of *Dictyostelium* dynein (Fig. 5B) and might make sliding more favourable.

Change in dynein affinity for microtubules

How stalk sliding lowers the affinity of dynein for microtubules was recently revealed by a 9-Å-resolution cryo-EM structure of the MTBD bound to microtubules (Redwine et al., 2012). The authors used their EM data and molecular dynamics simulations to determine how the bound MTBD differs from that in the X-ray crystal structure of the low-affinity form (Carter et al., 2008). In the high-affinity form, the MTBD interacts with microtubules through three α-helices (H1, H3 and H6), whereas in the low-affinity MTBD, CC1 sliding moves H1 and H3 relative to H6 and breaks the electrostatic interactions the helices make with the microtubule (Fig. 5C).

Conformational changes in the AAA+ ring drive stalk sliding

There is currently no indication of the exact mechanism through which changes in the AAA+ ring trigger sliding of the helices in the stalk. It is possible, however, to speculate on the underlying molecular events. As AAA1 opens and closes, the largest movements between AAA+ domains are observed to occur around those that are connected to the stalk and buttress (supplementary material Movies 1, 2). The full closure of AAA1 upon ATP binding is likely to result in additional movements of the AAA+ domains compared with those observed so far. This might strain the interaction between the stalk and buttress and trigger a conformational change in the stalk. The buttress interacts with the stalk immediately next to two highly conserved residues; a tryptophan residue (Trp) in CC2 that is directly opposite a glycine residue (Gly) in CC1 (Fig. 5D). Tryptophan is a bulky aromatic residue that is difficult to fit into the core of the coiled-coil, whereas glycine is poor at forming

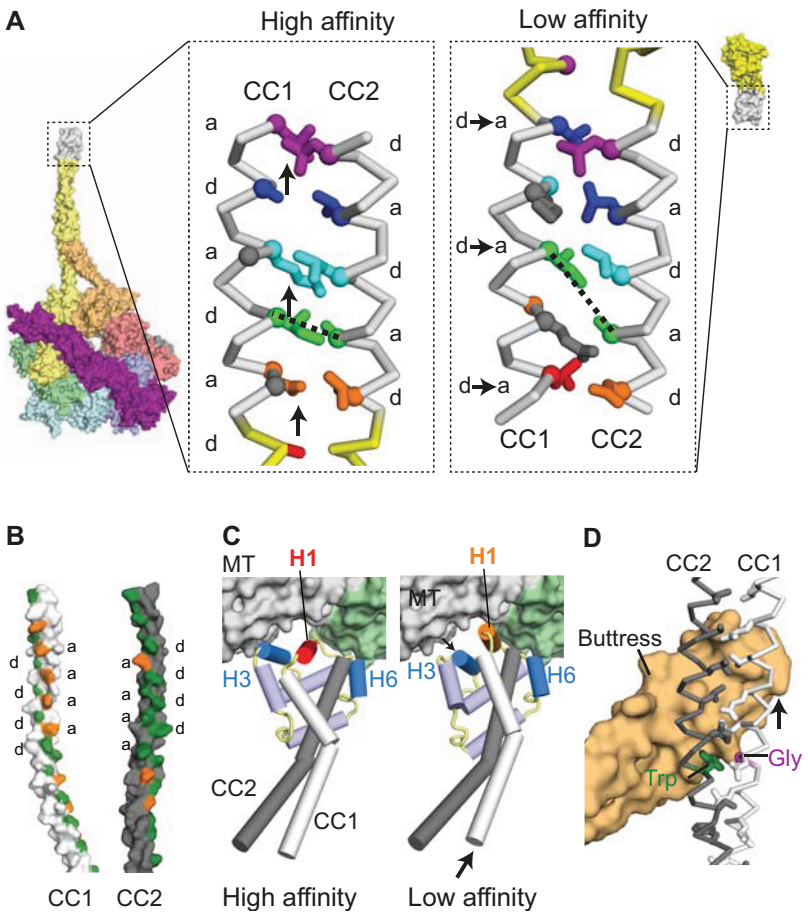

Fig. 5. Communication in the dynein stalk. (**A**) The dynein coiled-coil stalk can exist in two states. One helix (CC1) slides with respect to the second helix by half of a heptad repeat (see text for full description). The half-heptad sliding mechanism is likely to be responsible for the communication between the AAA+ ring and the microtubule binding domain (MTBD). Left: the structure of the top of the truncated stalk from the *Dictyostelium* motor domain (PDB ID 3VKG), which is expected to be in the high-affinity conformation. Residues that pack in the core of the coiled-coil are shown in stick representation and are coloured. Their position in the coiled-coil heptad repeat is marked by 'a' or 'd'. Right: the structure of the mouse MTBD (yellow) and part of the stalk (grey) trapped in a low-affinity conformation (PDB ID 3ERR). The equivalent residues are coloured as for the high-affinity structure. CC1 has slid by half a heptad toward the MTBD (see slope of the broken line). Residues previously in the 'd' position in CC1 have moved into the 'a' position. Residues previously in the 'a' position have moved out of the core (coloured, but represented as spheres). Residues previously outside the core (grey) have moved into the 'd' positions. (**B**) A conserved pattern of hydrophilic residues in the core of the dynein stalk may facilitate CC1 sliding. The two helices of the *Dictyostelium* stalk have been separated and the residues in the 'a' and 'd' positions of the heptad repeat are coloured according to their hydrophobicity. In CC1, residues in the 'd' position are consistently hydrophobic, whereas those in the 'a' position are consistently hydrophilic (orange). In CC2, most residues in the coiled-coil core are hydrophobic. (**C**) Changing the affinity of dynein for microtubules. Left: a model of the high-affinity form of the MTBD that is based on a 9-Å cryo-EM structure is shown (PDB ID 1J1T). Right: model of the low-affinity form of the MTBD next to a microtubule (PDB ID 1J1U, based on crystal structure 3ERR). Sliding of CC1 (arrow) rearranges the MTBD, so that helices H1, H3 and H6 are no long all able to contact the microtubule. (**D**) The buttress interacts with the base of the stalk, just above a universally conserved tryptophan (Trp) and glycine (Gly) residue in CC2 and CC1, respectively. Rotation of the tryptophan residue deeper into the core of the coiled-coil and melting of CC1 at the glycine residue might account for the sliding motion of CC1 (arrow).

α-helices and might cause CC1 to unwind. Changes in the stalk–buttress interaction might therefore push the tryptophan into the core of the coiled-coil and cause CC1 to melt at the glycine residue and shift outwards towards the MTBD. However, elucidating exactly how movements of the AAA+ ring are communicated to the base of the stalk will require a high-resolution crystal structure of the motor domain in the ATP-bound conformation.

Processive motion of cytoplasmic dynein dimers

A number of cytoskeletal motor proteins, including cytoplasmic dynein (King and Schroer, 2000; Reck-Peterson et al., 2006; Ross et al., 2006; Toba et al., 2006) are processive motors, taking multiple steps along their track before detaching. Conventional kinesin and myosin V are processive because the ATP hydrolysis cycles that occur in the two motor domains in the dimer are tightly coupled (a process also called gating). Gating ensures that the cycle of ATP hydrolysis in one motor domain can only continue when the other motor domain has stepped past it (Higuchi and Endow, 2002). The walking mechanism of dynein is different, and is only weakly coupled. Studies using high-precision tracking of single dimeric yeast dynein molecules, in which each motor domain is labelled with a differently coloured fluorescent group, suggest that the two motor domains do not

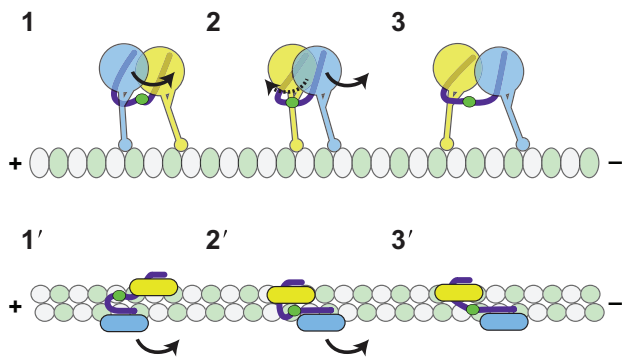

Fig. 6. Walking model for a dynein dimer. The upper panel shows a representation of the walking of a dimerized pair of dynein motor domains attached to the microtubule and viewed from the side. Both motor domains are in a post-powerstroke conformation, with the yellow motor domain in front of the blue one (1). The linker domains are shown in purple and are on the rear side of each motor domain in this view. The site of dimerization is represented by a green oval. Following this, the blue motor domain has swung past the yellow motor domain to take the lead (2). If the blue (leading) motor domain moves again it is almost as likely to move forward as it is to move backwards (broken arrow). Next, the blue motor domain has undergone a second (non-alternating, non-passing) forwards step (3); it detached from the microtubule, rebound in a forward position and has returned to the post-powerstroke conformation. The yellow (lagging) motor domain is more likely to step forwards as the distance between the motor domains increases. The lower panel shows the same stages of movement as described above (1–3), but they are now viewed from above (1′–3′).

need to move alternately (DeWitt et al., 2012; Qiu et al., 2012). Either of the two motor domains can take multiple steps without the other one moving, with the leading head being able to take multiple steps out in front before the lagging head catches up (Fig. 6). The two dynein motor domains move by a mixture of alternating and non-alternating steps, and passing and non-passing movements.

Processive movement in dynein does not, therefore, absolutely require the coordination between the ATPase cycles of the two motor domains. Instead, the walking mechanism is probably related to a high duty ratio (Shima et al., 2006a) in which the time a motor domain is detached from the microtubule is sufficiently short so that it is unlikely that the other head will detach. It has been shown that myosins that have been engineered to remove their gating mechanism can move processively by a high duty ratio alone (Elting et al., 2011).

Although either motor domain in a dynein dimer can move either forwards or backwards at each step, the overall direction of the motor is biased forwards, towards the minus end of the microtubule. The leading motor domain can move forwards or backwards with only a small bias for the forward direction (55% versus 45%), but the lagging motor-domain is much more likely to move forwards (DeWitt et al., 2012). In addition, as the spacing between the motor domains increases, the probability that the lagging head also moves increases (DeWitt et al., 2012; Qiu et al., 2012). The powerstroke of the linker domain occurs shortly after the motor domain rebinds and its role is not to throw the other motor domain forwards (the powerstroke can occur on either leading or lagging motor domain) but rather to generate tension between the two motor-domains, which increases the chance that the lagging head will catch up with the leader. The mechanism by which the lagging head tends to catch up is likely to be an intrinsic feature of the MTBD (Carter et al., 2008), which requires less force to pull it forwards than backwards (Gennerich et al., 2007).

Conclusions

Dynein uses a number of distinctive mechanisms to generate motility. Similar to other AAA+ proteins, it uses the opening and closing of the AAA1 ATP-binding site to bring a set of conserved inserts into contact with the linker, which remodel it into the pre-powerstroke position. The closing of the AAA1 site drives multiple movements between the other AAA+ domains in the ring, as illustrated by the comparison of the nucleotide-free and ADP-bound motor domain structures. These changes are likely to be coupled directly to the movement that occurs between the buttress and stalk, which drives a shift in the register in the coiled-coil stalk and communicates ATP-mediated conformational changes to the MTBD. Even at the level of processive movement, dynein behaves differently from the other cytoskeletal motors, as it appears to use a high duty ratio mechanism to achieve processivity.

To function in the cell, dynein motor activity is likely to be closely regulated. Regulation of axonemal dynein motor activity controls both the beat frequency and waveform of cilia and flagella (Salathe, 2007; Wirschell et al., 2011). Regulation of cytoplasmic dynein motor activity involves both the dynein tail and regulatory factors, such as dynactin and Lis1. Regulation and specific targeting of cytoplasmic dynein allow this one motor protein complex to carry out many different functions. A full understanding of the structural basis of dynein movement will be vital to determine how the motor regulation works.

Acknowledgements

I thank H. Schmidt, R. McKenney, S. Reck-Peterson, S. Bullock, M. Carter, L. Leake, J. Pennell, A. Roberts and A. Diamant, for their invaluable comments on the manuscript.

Funding

The work of my laboratory is supported by the UK Medical Research Council [MRC file reference number MC_UP_A025_1011].

Supplementary material available online at
http://jcs.biologists.org/lookup/suppl/doi:10.1242/jcs.120725/-/DC1

References

Allan, V. J. (2011). Cytoplasmic dynein. *Biochem. Soc. Trans.* **39**, 1169-1178.
Bassler, J., Kallas, M., Pertschy, B., Ulbrich, C., Thoms, M. and Hurt, E. (2010). The AAA-ATPase Rea1 drives removal of biogenesis factors during multiple stages of 60S ribosome assembly. *Mol. Cell* **38**, 712-721.
Bochtler, M., Hartmann, C., Song, H. K., Bourenkov, G. P., Bartunik, H. D. and Huber, R. (2000). The structures of HsIU and the ATP-dependent protease HsIU-HsIV. *Nature* **403**, 800-805.
Burgess, S. A., Walker, M. L., Sakakibara, H., Knight, P. J. and Oiwa, K. (2003). Dynein structure and power stroke. *Nature* **421**, 715-718.
Carter, A. P. and Vale, R. D. (2010). Communication between the AAA+ ring and microtubule-binding domain of dynein. *Biochem. Cell Biol.* **88**, 15-21.
Carter, A. P., Garbarino, J. E., Wilson-Kubalek, E. M., Shipley, W. E., Cho, C., Milligan, R. A., Vale, R. D. and Gibbons, I. R. (2008). Structure and functional role of dynein's microtubule-binding domain. *Science* **322**, 1691-1695.
Carter, A. P., Cho, C., Jin, L. and Vale, R. D. (2011). Crystal structure of the dynein motor domain. *Science* **331**, 1159-1165.
Cho, C. and Vale, R. D. (2012). The mechanism of dynein motility: insight from crystal structures of the motor domain. *Biochim. Biophys. Acta* **1823**, 182-191.
Cho, C., Reck-Peterson, S. L. and Vale, R. D. (2008). Regulatory ATPase sites of cytoplasmic dynein affect processivity and force generation. *J. Biol. Chem.* **283**, 25839-25845.
Cole, D. G. (2003). The intraflagellar transport machinery of Chlamydomonas reinhardtii. *Traffic* **4**, 435-442.

Croasdale, R., Ivins, F. J., Muskett, F., Daviter, T., Scott, D. J., Hardy, T., Smerdon, S. J., Fry, A. M. and Pfuhl, M. (2011). An undecided coiled coil: the leucine zipper of Nek2 kinase exhibits atypical conformational exchange dynamics. *J. Biol. Chem.* **286**, 27537-27547.

DeWitt, M. A., Chang, A. Y., Combs, P. A. and Yildiz, A. (2012). Cytoplasmic dynein moves through uncoordinated stepping of the AAA+ ring domains. *Science* **335**, 221-225.

Egan, M. J., Tan, K. and Reck-Peterson, S. L. (2012). Lis1 is an initiation factor for dynein-driven organelle transport. *J. Cell Biol.* **197**, 971-982.

Elting, M. W., Bryant, Z., Liao, J. C. and Spudich, J. A. (2011). Detailed tuning of structure and intramolecular communication are dispensable for processive motion of myosin VI. *Biophys. J.* **100**, 430-439.

Erzberger, J. P. and Berger, J. M. (2006). Evolutionary relationships and structural mechanisms of AAA+ proteins. *Annu. Rev. Biophys. Biomol. Struct.* **35**, 93-114.

Gee, M. A., Heuser, J. E. and Vallee, R. B. (1997). An extended microtubule-binding structure within the dynein motor domain. *Nature* **390**, 636-639.

Gennerich, A., Carter, A. P., Reck-Peterson, S. L. and Vale, R. D. (2007). Force-induced bidirectional stepping of cytoplasmic dynein. *Cell* **131**, 952-965.

Gibbons, I. R., Garbarino, J. E., Tan, C. E., Reck-Peterson, S. L., Vale, R. D. and Carter, A. P. (2005). The affinity of the dynein microtubule-binding domain is modulated by the conformation of its coiled-coil stalk. *J. Biol. Chem.* **280**, 23960-23965.

Glynn, S. E., Martin, A., Nager, A. R., Baker, T. A. and Sauer, R. T. (2009). Structures of asymmetric ClpX hexamers reveal nucleotide-dependent motions in a AAA+ protein-unfolding machine. *Cell* **139**, 744-756.

Grum, V. L., Li, D., MacDonald, R. I. and Mondragón, A. (1999). Structures of two repeats of spectrin suggest models of flexibility. *Cell* **98**, 523-535.

Higuchi, H. and Endow, S. A. (2002). Directionality and processivity of molecular motors. *Curr. Opin. Cell Biol.* **14**, 50-57.

Huang, J., Roberts, A. J., Leschziner, A. E. and Reck-Peterson, S. L. (2012). Lis1 acts as a "clutch" between the ATPase and microtubule-binding domains of the dynein motor. *Cell* **150**, 975-986.

Imamula, K., Kon, T., Ohkura, R. and Sutoh, K. (2007). The coordination of cyclic microtubule association/dissociation and tail swing of cytoplasmic dynein. *Proc. Natl. Acad. Sci. USA* **104**, 16134-16139.

Kardon, J. R. and Vale, R. D. (2009). Regulators of the cytoplasmic dynein motor. *Nat. Rev. Mol. Cell Biol.* **10**, 854-865.

King, S. J. and Schroer, T. A. (2000). Dynactin increases the processivity of the cytoplasmic dynein motor. *Nat. Cell Biol.* **2**, 20-24.

Kon, T., Nishiura, M., Ohkura, R., Toyoshima, Y. Y. and Sutoh, K. (2004). Distinct functions of nucleotide-binding/hydrolysis sites in the four AAA modules of cytoplasmic dynein. *Biochemistry* **43**, 11266-11274.

Kon, T., Mogami, T., Ohkura, R., Nishiura, M. and Sutoh, K. (2005). ATP hydrolysis cycle-dependent tail motions in cytoplasmic dynein. *Nat. Struct. Mol. Biol.* **12**, 513-519.

Kon, T., Imamula, K., Roberts, A. J., Ohkura, R., Knight, P. J., Gibbons, I. R., Burgess, S. A. and Sutoh, K. (2009). Helix sliding in the stalk coiled coil of dynein couples ATPase and microtubule binding. *Nat. Struct. Mol. Biol.* **16**, 325-333.

Kon, T., Sutoh, K. and Kurisu, G. (2011). X-ray structure of a functional full-length dynein motor domain. *Nat. Struct. Mol. Biol.* **18**, 638-642.

Kon, T., Oyama, T., Shimo-Kon, R., Imamula, K., Shima, T., Sutoh, K. and Kurisu, G. (2012). The 2.8 Å crystal structure of the dynein motor domain. *Nature* **484**, 345-350.

Koonce, M. P. (1997). Identification of a microtubule-binding domain in a cytoplasmic dynein heavy chain. *J. Biol. Chem.* **272**, 19714-19718.

Kull, F. J., Vale, R. D. and Fletterick, R. J. (1998). The case for a common ancestor: kinesin and myosin motor proteins and G proteins. *J. Muscle Res. Cell Motil.* **19**, 877-886.

Macheboeuf, P., Buffalo, C., Fu, C. Y., Zinkernagel, A. S., Cole, J. N., Johnson, J. E., Nizet, V. and Ghosh, P. (2011). Streptococcal M1 protein constructs a pathological host fibrinogen network. *Nature* **472**, 64-68.

McKenney, R. J., Vershinin, M., Kunwar, A., Vallee, R. B. and Gross, S. P. (2010). LIS1 and NudE induce a persistent dynein force-producing state. *Cell* **141**, 304-314.

Miki, H., Okada, Y. and Hirokawa, N. (2005). Analysis of the kinesin superfamily: insights into structure and function. *Trends Cell Biol.* **15**, 467-476.

Neuwald, A. F., Aravind, L., Spouge, J. L. and Koonin, E. V. (1999). AAA+: A class of chaperone-like ATPases associated with the assembly, operation, and disassembly of protein complexes. *Genome Res.* **9**, 27-43.

Odronitz, F. and Kollmar, M. (2007). Drawing the tree of eukaryotic life based on the analysis of 2,269 manually annotated myosins from 328 species. *Genome Biol.* **8**, R196.

Qiu, W., Derr, N. D., Goodman, B. S., Villa, E., Wu, D., Shih, W. and Reck-Peterson, S. L. (2012). Dynein achieves processive motion using both stochastic and coordinated stepping. *Nat. Struct. Mol. Biol.* **19**, 193-200.

Rappas, M., Schumacher, J., Beuron, F., Niwa, H., Bordes, P., Wigneshweraraj, S., Keetch, C. A., Robinson, C. V., Buck, M. and Zhang, X. (2005). Structural insights into the activity of enhancer-binding proteins. *Science* **307**, 1972-1975.

Reck-Peterson, S. L., Yildiz, A., Carter, A. P., Gennerich, A., Zhang, N. and Vale, R. D. (2006). Single-molecule analysis of dynein processivity and stepping behavior. *Cell* **126**, 335-348.

Redwine, W. B., Hernández-López, R., Zou, S., Huang, J., Reck-Peterson, S. L. and Leschziner, A. E. (2012). Structural basis for microtubule binding and release by dynein. *Science* **337**, 1532-1536.

Roberts, A. J., Numata, N., Walker, M. L., Kato, Y. S., Malkova, B., Kon, T., Ohkura, R., Arisaka, F., Knight, P. J., Sutoh, K. et al. (2009). AAA+ Ring and linker swing mechanism in the dynein motor. *Cell* **136**, 485-495.

Roberts, A. J., Malkova, B., Walker, M. L., Sakakibara, H., Numata, N., Kon, T., Ohkura, R., Edwards, T. A., Knight, P. J., Sutoh, K. et al. (2012). ATP-driven remodeling of the linker domain in the dynein motor. *Structure* **20**, 1670-1680.

Ross, J. L., Wallace, K., Shuman, H., Goldman, Y. E. and Holzbaur, E. L. (2006). Processive bidirectional motion of dynein-dynactin complexes in vitro. *Nat. Cell Biol.* **8**, 562-570.

Salathe, M. (2007). Regulation of mammalian ciliary beating. *Annu. Rev. Physiol.* **69**, 401-422.

Samsó, M., Radermacher, M., Frank, J. and Koonce, M. P. (1998). Structural characterization of a dynein motor domain. *J. Mol. Biol.* **276**, 927-937.

Schmidt, H., Gleave, E. S. and Carter, A. P. (2012). Insights into dynein motor domain function from a 3.3-Å crystal structure. *Nat. Struct. Mol. Biol.* **19**, 492-497, S1.

Shima, T., Imamula, K., Kon, T., Ohkura, R. and Sutoh, K. (2006a). Head-head coordination is required for the processive motion of cytoplasmic dynein, an AAA+ molecular motor. *J. Struct. Biol.* **156**, 182-189.

Shima, T., Kon, T., Imamula, K., Ohkura, R. and Sutoh, K. (2006b). Two modes of microtubule sliding driven by cytoplasmic dynein. *Proc. Natl. Acad. Sci. USA* **103**, 17736-17740.

Smith, D. M., Fraga, H., Reis, C., Kafri, G. and Goldberg, A. L. (2011). ATP binds to proteasomal ATPases in pairs with distinct functional effects, implying an ordered reaction cycle. *Cell* **144**, 526-538.

Toba, S., Watanabe, T. M., Yamaguchi-Okimoto, L., Toyoshima, Y. Y. and Higuchi, H. (2006). Overlapping hand-over-hand mechanism of single molecular motility of cytoplasmic dynein. *Proc. Natl. Acad. Sci. USA* **103**, 5741-5745.

Vale, R. D. (2003). The molecular motor toolbox for intracellular transport. *Cell* **112**, 467-480.

Vale, R. D. and Milligan, R. A. (2000). The way things move: looking under the hood of molecular motor proteins. *Science* **288**, 88-95.

Vaughan, K. T. (2012). Roles of cytoplasmic dynein during mitosis. In *Dyneins: Structure, Biology and Disease* (ed. S. J. King), pp 523. Amsterdam; Boston: Academic Press.

Wendler, P., Ciniawsky, S., Kock, M. and Kube, S. (2012). Structure and function of the AAA+ nucleotide binding pocket. *Biochim. Biophys. Acta* **1823**, 2-14.

Wickstead, B. and Gull, K. (2007). Dyneins across eukaryotes: a comparative genomic analysis. *Traffic* **8**, 1708-1721.

Wirschell, M., Yamamoto, R., Alford, L., Gokhale, A., Gaillard, A. and Sale, W. S. (2011). Regulation of ciliary motility: conserved protein kinases and phosphatases are targeted and anchored in the ciliary axoneme. *Arch. Biochem. Biophys.* **510**, 93-100.